

# Fano factor, $\Delta T$ -noise and cross-correlations in double quantum dots

A. Crépieux,<sup>1</sup> T.Q. Duong,<sup>1</sup> and M. Lavagna<sup>2</sup>

<sup>1</sup>*Aix Marseille Univ, Université de Toulon, CNRS, CPT, Marseille, France*

<sup>2</sup>*Univ. Grenoble Alpes, CEA, INAC, PHELIQS, F-38000 Grenoble, France*

(Dated: June 6, 2023)

We present a theoretical study of electrical current fluctuations and finite-frequency noise in a double quantum dot connected to two electron reservoirs with the aim of deriving the Fano factor, the  $\Delta T$ -noise and the cross-correlations. This allows one to highlight several interesting features. Firstly the possibility of getting a significant reduction of current noise and Fano factor either when the system is placed in a given operating regime, or when a temperature gradient is applied between the two reservoirs, resulting from the fact that a negative  $\Delta T$ -noise is generated. The second feature is the sign change found in the cross-correlator between the two reservoirs with increasing frequencies. This study clarifies the understanding of the results obtained experimentally in such systems.

*Introduction* – The reduction of electrical noise in double quantum dots is a major issue if one wishes to finely control the electric charge transfer and improve the performance and the quality factor, in spin-qubits in particular[1–3]. There are some theoretical studies devoted to the characterization of current fluctuations and electrical noise in double quantum dots[4], but they are most often limited to the calculation of noise at zero frequency[5–18] or use perturbative approaches[19–21] based mainly on master equation technique. However we now have experimental works studying fluctuations in double quantum dots, built from GaAs/AlGaAs or Si/SiGe heterostructures, that are expected to undergo a considerable development in the coming years. Part of these works are looking for the optimal conditions to suppress the sensitivity of the device to electrical noise, in order to obtain long-lived and high-fidelity spin qubits[1–3], while others are devoted to the measurement of electrical current cross-correlations[22] or to the measurement of entropy fluctuations[23]. All these experimental works provide the motivation for developing further theoretical studies of electrical noise and current fluctuations in double quantum dots.

In this letter, we present a non-perturbative approach to determine the finite-frequency noise in a double quantum dot system using the non-equilibrium Green function technique. After outlining the formalism used to model the double quantum dot connected to left and right electron reservoirs, we give the results for the general expression of the noise. We numerically calculate the noise and the Fano factor in various geometries: double quantum dot connected either in series or in parallel, and discuss the results. We next focus our interest to the  $\Delta T$ -noise produced when the two reservoirs are raised to different temperatures[24–29]. We show that the latter quantity exhibits specific characteristics in its evolution[30] that have never been demonstrated before in double quantum dots. To end up, we determine the cross-correlator between the left and right reservoirs and compare the obtained results with the experimental ones [22].

*Model and results* – The Hamiltonian of two coupled quantum dots connected to left (L) and right (R) reservoirs is given by

$$\begin{aligned} \hat{\mathcal{H}} = & \sum_{\substack{\alpha=L,R \\ k \in \alpha}} \varepsilon_{\alpha k} \hat{c}_{\alpha k}^\dagger \hat{c}_{\alpha k} + \sum_{\substack{i=1,2 \\ n \in i}} \varepsilon_{in} \hat{d}_{in}^\dagger \hat{d}_{in} \\ & + \sum_{\substack{n \in 1 \\ m \in 2}} \mathcal{V}_{12} \hat{d}_{2m}^\dagger \hat{d}_{1n} + \sum_{\substack{\alpha=L,R \\ k \in \alpha}} \sum_{\substack{i=1,2 \\ n \in i}} V_{i\alpha} \hat{c}_{\alpha k}^\dagger \hat{d}_{in} + h.c. \end{aligned} \quad (1)$$

where  $\hat{c}_{\alpha k}^\dagger$  ( $\hat{c}_{\alpha k}$ ) is the creation (annihilation) operator related to the reservoir  $\alpha$  with momentum  $k$  and energy  $\varepsilon_{\alpha k}$ , and  $\hat{d}_{in}^\dagger$  ( $\hat{d}_{in}$ ) is the creation (annihilation) operator related to the dot  $i$ , with  $i = 1, 2$ . Each dot  $i$  contains  $N$  discrete energy levels denoted  $\varepsilon_{in}$ , with  $n \in [1, N]$ . The notation *h.c.* corresponds to the hermitian conjugate terms associated with the third and fourth contributions in Eq. (1). One assumes that the inter-dot coupling  $\mathcal{V}_{12}$  between the states  $|1n\rangle$  and  $|2m\rangle$  in the dots, and the hopping integral  $V_{i\alpha}$  between the states  $|in\rangle$  in the dot  $i$  and  $|\alpha k\rangle$  in the reservoir  $\alpha$  do not depend on the indices  $n$  and  $m$ , nor on the momentum  $k$ .

The finite-frequency non-symmetrized noise in the DQD is defined as the Fourier transform of the current fluctuations,  $\mathcal{S}_{\alpha\beta}(\omega) = \int_{-\infty}^{\infty} \langle \Delta \hat{I}_\alpha(t) \Delta \hat{I}_\beta(0) \rangle e^{-i\omega t} dt$ , where  $\Delta \hat{I}_\alpha(t) = \hat{I}_\alpha(t) - \langle \hat{I}_\alpha \rangle$  is the deviation of the current  $\hat{I}_\alpha(t)$  from its average value  $\langle \hat{I}_\alpha \rangle$ . The calculations lead to the expression  $\mathcal{S}_{\alpha\beta}(\omega) = \frac{e^2}{h} \sum_{i=1}^5 \int_{-\infty}^{\infty} \text{Tr} \{ \underline{\underline{\mathcal{C}}}_{\alpha\beta}^{(i)} \} d\varepsilon$ , where  $\text{Tr} \{ \}$  corresponds to the trace, and where the matrices  $\underline{\underline{\mathcal{C}}}_{\alpha\beta}^{(i)}$  are given by

$$\begin{aligned} \underline{\underline{\mathcal{C}}}_{\alpha\beta}^{(i)} = & \delta_{\alpha\beta} \left[ \underline{\underline{\mathbf{G}}}^<(\varepsilon) \underline{\underline{\Sigma}}_\alpha^>(\varepsilon - \hbar\omega) \right. \\ & \left. + \underline{\underline{\mathbf{G}}}^>(\varepsilon - \hbar\omega) \underline{\underline{\Sigma}}_\alpha^<(\varepsilon) \right], \end{aligned} \quad (2)$$

$$\begin{aligned} \underline{\underline{C}}_{\alpha\beta}^{(2)} = & - \left[ \underline{\underline{\mathbf{G}}}^r(\varepsilon - \hbar\omega) \underline{\underline{\Sigma}}_{\beta}^>(\varepsilon - \hbar\omega) \right. \\ & \left. + \underline{\underline{\mathbf{G}}}^>(\varepsilon - \hbar\omega) \underline{\underline{\Sigma}}_{\beta}^a(\varepsilon - \hbar\omega) \right] \\ & \times \left[ \underline{\underline{\mathbf{G}}}^r(\varepsilon) \underline{\underline{\Sigma}}_{\alpha}^<(\varepsilon) + \underline{\underline{\mathbf{G}}}^<(\varepsilon) \underline{\underline{\Sigma}}_{\alpha}^a(\varepsilon) \right], \quad (3) \end{aligned}$$

$$\begin{aligned} \underline{\underline{C}}_{\alpha\beta}^{(3)} = & \underline{\underline{\mathbf{G}}}^>(\varepsilon - \hbar\omega) \left[ \underline{\underline{\Sigma}}_{\beta}^<(\varepsilon) \underline{\underline{\mathbf{G}}}^a(\varepsilon) \underline{\underline{\Sigma}}_{\alpha}^a(\varepsilon) \right. \\ & \left. + \underline{\underline{\Sigma}}_{\beta}^r(\varepsilon) \underline{\underline{\mathbf{G}}}^<(\varepsilon) \underline{\underline{\Sigma}}_{\alpha}^a(\varepsilon) + \underline{\underline{\Sigma}}_{\beta}^r(\varepsilon) \underline{\underline{\mathbf{G}}}^r(\varepsilon) \underline{\underline{\Sigma}}_{\alpha}^<(\varepsilon) \right], \quad (4) \end{aligned}$$

$$\begin{aligned} \underline{\underline{C}}_{\alpha\beta}^{(4)} = & \underline{\underline{\mathbf{G}}}^<(\varepsilon) \left[ \underline{\underline{\Sigma}}_{\alpha}^r(\varepsilon - \hbar\omega) \underline{\underline{\mathbf{G}}}^r(\varepsilon - \hbar\omega) \underline{\underline{\Sigma}}_{\beta}^>(\varepsilon - \hbar\omega) \right. \\ & \left. + \underline{\underline{\Sigma}}_{\alpha}^r(\varepsilon - \hbar\omega) \underline{\underline{\mathbf{G}}}^>(\varepsilon - \hbar\omega) \underline{\underline{\Sigma}}_{\beta}^a(\varepsilon - \hbar\omega) \right. \\ & \left. + \underline{\underline{\Sigma}}_{\alpha}^>(\varepsilon - \hbar\omega) \underline{\underline{\mathbf{G}}}^a(\varepsilon - \hbar\omega) \underline{\underline{\Sigma}}_{\beta}^a(\varepsilon - \hbar\omega) \right], \quad (5) \end{aligned}$$

and,

$$\begin{aligned} \underline{\underline{C}}_{\alpha\beta}^{(5)} = & - \left[ \underline{\underline{\Sigma}}_{\alpha}^r(\varepsilon - \hbar\omega) \underline{\underline{\mathbf{G}}}^>(\varepsilon - \hbar\omega) \right. \\ & \left. + \underline{\underline{\Sigma}}_{\alpha}^>(\varepsilon - \hbar\omega) \underline{\underline{\mathbf{G}}}^a(\varepsilon - \hbar\omega) \right] \\ & \times \left[ \underline{\underline{\Sigma}}_{\beta}^r(\varepsilon) \underline{\underline{\mathbf{G}}}^<(\varepsilon) + \underline{\underline{\Sigma}}_{\beta}^<(\varepsilon) \underline{\underline{\mathbf{G}}}^a(\varepsilon) \right]. \quad (6) \end{aligned}$$

The self-energy matrices associated with the reservoir  $\alpha$  are given by  $\underline{\underline{\Sigma}}_{\alpha}^{r,a}(\varepsilon) = \mp(i/2)\underline{\underline{\Gamma}}_{\alpha}$ ,  $\underline{\underline{\Sigma}}_{\alpha}^<(\varepsilon) = if_{\alpha}^e(\varepsilon)\underline{\underline{\Gamma}}_{\alpha}$  and  $\underline{\underline{\Sigma}}_{\alpha}^>(\varepsilon) = -if_{\alpha}^h(\varepsilon)\underline{\underline{\Gamma}}_{\alpha}$ , where  $f_{\alpha}^e(\varepsilon) = 1/(1 + \exp(\varepsilon - \mu_{\alpha})/k_B T_{\alpha})$  and  $f_{\alpha}^h(\varepsilon) = 1 - f_{\alpha}^e(\varepsilon)$  are the Fermi-Dirac distribution functions for electrons and holes respectively,  $T_{\alpha}$  is the temperature and  $\mu_{\alpha}$  the chemical potential of the reservoir  $\alpha$  with density of states  $\rho_{\alpha}$ , which is energy independent in the wide-band limit, and where the elements of the dot-reservoir coupling matrix  $\underline{\underline{\Gamma}}_{\alpha}$  are  $\Gamma_{\alpha,ij} = 2\pi\rho_{\alpha}V_{i\alpha}^*V_{j\alpha}$ . The retarded Green function associated with the double quantum dot is a  $2 \times 2$  matrix given by[31]

$$\underline{\underline{\mathbf{G}}}^r(\varepsilon) = \frac{1}{D^r(\varepsilon)} \begin{pmatrix} \tilde{\mathbf{g}}_1^r(\varepsilon) & \tilde{\mathbf{g}}_1^r(\varepsilon)\tilde{\underline{\underline{\Sigma}}}_{12}^r(\varepsilon)\tilde{\mathbf{g}}_2^r(\varepsilon) \\ \tilde{\mathbf{g}}_2^r(\varepsilon)\tilde{\underline{\underline{\Sigma}}}_{21}^r(\varepsilon)\tilde{\mathbf{g}}_1^r(\varepsilon) & \tilde{\mathbf{g}}_2^r(\varepsilon) \end{pmatrix},$$

where  $D^r(\varepsilon) = 1 - \tilde{\mathbf{g}}_1^r(\varepsilon)\tilde{\underline{\underline{\Sigma}}}_{12}^r(\varepsilon)\tilde{\mathbf{g}}_2^r(\varepsilon)\tilde{\underline{\underline{\Sigma}}}_{21}^r(\varepsilon)$  and  $\tilde{\mathbf{g}}_i^r(\varepsilon) = \mathbf{g}_i^r(\varepsilon)/(1 - \tilde{\underline{\underline{\Sigma}}}_{ii}^r(\varepsilon)\mathbf{g}_i^r(\varepsilon))$ . In these expressions appear the retarded Green function of the disconnected dot  $i$ , defined as  $\mathbf{g}_i^r(\varepsilon) = \sum_{n \in i} g_{in}^r(\varepsilon)$  with  $g_{in}^r(\varepsilon) = 1/(\varepsilon - \varepsilon_{in} + i0^+)$ , and the total self-energy:  $\tilde{\underline{\underline{\Sigma}}}^r(\varepsilon) = \sum_{\alpha=L,R} \underline{\underline{\Sigma}}_{\alpha}^r(\varepsilon) + \underline{\underline{\Sigma}}_{\text{int}}^r$ , where the matrix  $\underline{\underline{\Sigma}}_{\text{int}}^r$  is given by

$$\underline{\underline{\Sigma}}_{\text{int}}^r = \begin{pmatrix} 0 & \mathcal{V}_{12}^* \\ \mathcal{V}_{21}^* & 0 \end{pmatrix}. \quad (8)$$

The advanced Green function matrix  $\underline{\underline{\mathbf{G}}}^a(\varepsilon)$  is obtained from the retarded one by replacing the superscript  $r$  by the superscript  $a$  in the expression giving  $\underline{\underline{\mathbf{G}}}^r(\varepsilon)$ . Moreover, one has  $\underline{\underline{\mathbf{G}}}^{\lessgtr}(\varepsilon) = \sum_{\alpha=L,R} \underline{\underline{\mathbf{G}}}^r(\varepsilon) \underline{\underline{\Sigma}}_{\alpha}^{\lessgtr}(\varepsilon) \underline{\underline{\mathbf{G}}}^a(\varepsilon)$ .

We have established the following expression for the auto-correlator  $\mathcal{S}_{LL}(\omega)$  calculated in the  $L$ -reservoir

$$\begin{aligned} \mathcal{S}_{LL}(\omega) = & \frac{e^2}{h} \int_{-\infty}^{\infty} d\varepsilon \text{Tr} \left\{ f_L^e(\varepsilon) f_L^h(\varepsilon - \hbar\omega) \right. \\ & \times \left[ \underline{\underline{\mathcal{T}}}_{LL}^{\text{eff}}(\varepsilon) \underline{\underline{\mathcal{T}}}_{LL}^{\text{eff}}(\varepsilon - \hbar\omega) + \left| t_{LL}(\varepsilon) - \underline{\underline{t}}_{LL}(\varepsilon - \hbar\omega) \right|^2 \right] \\ & + f_R^e(\varepsilon) f_R^h(\varepsilon - \hbar\omega) \underline{\underline{\mathcal{T}}}_{RL}(\varepsilon) \underline{\underline{\mathcal{T}}}_{RL}(\varepsilon - \hbar\omega) \\ & + f_L^e(\varepsilon) f_R^h(\varepsilon - \hbar\omega) \left[ 1 - \underline{\underline{\mathcal{T}}}_{LL}^{\text{eff}}(\varepsilon) \right] \underline{\underline{\mathcal{T}}}_{RL}(\varepsilon - \hbar\omega) \\ & \left. + f_R^e(\varepsilon) f_L^h(\varepsilon - \hbar\omega) \underline{\underline{\mathcal{T}}}_{RL}(\varepsilon) \left[ 1 - \underline{\underline{\mathcal{T}}}_{LL}^{\text{eff}}(\varepsilon - \hbar\omega) \right] \right\}, \quad (9) \end{aligned}$$

where we have defined the transmission amplitude matrix  $\underline{\underline{t}}_{\alpha\alpha}(\varepsilon) = i\underline{\underline{\mathbf{G}}}^r(\varepsilon)\underline{\underline{\Gamma}}_{\alpha}$ , the transmission coefficient matrix  $\underline{\underline{\mathcal{T}}}_{\alpha\beta}(\varepsilon) = \underline{\underline{\mathbf{G}}}^r(\varepsilon)\underline{\underline{\Gamma}}_{\alpha}\underline{\underline{\mathbf{G}}}^a(\varepsilon)\underline{\underline{\Gamma}}_{\beta}$ , and the effective transmission coefficient matrix  $\underline{\underline{\mathcal{T}}}_{\alpha\alpha}^{\text{eff}}(\varepsilon) = \underline{\underline{t}}_{\alpha\alpha}(\varepsilon) + \underline{\underline{t}}_{\alpha\alpha}^+(\varepsilon) - \underline{\underline{\mathcal{T}}}_{\alpha\alpha}(\varepsilon)$ , where  $\underline{\underline{t}}_{\alpha\alpha}^+(\varepsilon)$  is the conjugate transpose of  $\underline{\underline{t}}_{\alpha\alpha}(\varepsilon)$ . The (7)expression for the cross-correlator  $\mathcal{S}_{LR}(\omega)$  is given by

$$\begin{aligned} \mathcal{S}_{LR}(\omega) = & \frac{e^2}{h} \int_{-\infty}^{\infty} d\varepsilon \text{Tr} \left\{ f_L^e(\varepsilon) f_L^h(\varepsilon - \hbar\omega) \left[ \left[ \underline{\underline{\mathcal{T}}}_{LL}(\varepsilon) - \underline{\underline{t}}_{LL}(\varepsilon) \right] \underline{\underline{\mathcal{T}}}_{LR}(\varepsilon - \hbar\omega) - \underline{\underline{\mathcal{T}}}_{LL}(\varepsilon) \underline{\underline{t}}_{RR}^+(\varepsilon - \hbar\omega) \right] \right. \\ & + f_R^e(\varepsilon) f_R^h(\varepsilon - \hbar\omega) \left[ \left[ \underline{\underline{\mathcal{T}}}_{RL}(\varepsilon) - \underline{\underline{t}}_{LL}^+(\varepsilon) \right] \underline{\underline{\mathcal{T}}}_{RR}(\varepsilon - \hbar\omega) - \underline{\underline{\mathcal{T}}}_{RL}(\varepsilon) \underline{\underline{t}}_{RR}(\varepsilon - \hbar\omega) \right] \\ & + f_L^e(\varepsilon) f_R^h(\varepsilon - \hbar\omega) \left[ \underline{\underline{\mathcal{T}}}_{LL}(\varepsilon) - \underline{\underline{t}}_{LL}(\varepsilon) \right] \left[ \underline{\underline{\mathcal{T}}}_{RR}(\varepsilon - \hbar\omega) - \underline{\underline{t}}_{RR}(\varepsilon - \hbar\omega) \right] \\ & \left. + f_R^e(\varepsilon) f_L^h(\varepsilon - \hbar\omega) \left[ \underline{\underline{\mathcal{T}}}_{RL}(\varepsilon) - \underline{\underline{t}}_{LL}^+(\varepsilon) \right] \left[ \underline{\underline{\mathcal{T}}}_{LR}(\varepsilon - \hbar\omega) - \underline{\underline{t}}_{RR}^+(\varepsilon - \hbar\omega) \right] \right\}. \quad (10) \end{aligned}$$

The auto-correlator  $\mathcal{S}_{RR}(\omega)$  and cross-correlator  $\mathcal{S}_{RL}(\omega)$  are obtained by interchanging the indices  $L$  and  $R$  in Eq. (9) and Eq. (10), respectively. These results are a generalization to double quantum dots of the results obtained for a single dot[32, 33]. The main differences are the expressions themselves of the Green functions and of the transmission amplitudes and coefficients, and the presence of matrix products rather than scalar products. Eqs. (9) and (10) apply for both serial and parallel double quantum dots since one can freely play with the values of the dot-reservoir couplings  $\Gamma_{\alpha,ij}$ . In the following we consider only symmetrical dot-reservoir couplings, meaning that  $\Gamma \equiv \Gamma_{L,11} = \Gamma_{R,22}$  and  $\Gamma_{L,22} = \Gamma_{R,11} = 0$  for a serial double dot, and  $\Gamma \equiv \Gamma_{\alpha,ij}, \forall \{\alpha, i, j\}$ , for a parallel double dot.

*Discussion* – We first study the Fano factor, defined as  $\mathcal{F}_\alpha = \mathcal{S}_{\alpha\alpha}(0)/(eI_\alpha)$ , in order to identify the regions where the zero-frequency noise is reduced compared to the current, i.e. such that one has  $\mathcal{F}_\alpha \ll 1$ . Figure 1 displays the color-scale plot of the Fano factor associated to the L-reservoir,  $\mathcal{F}_L$ , as a function of bias voltage  $V = \mu_L - \mu_R$  and detuning energy  $\varepsilon_d = \varepsilon_2 - \varepsilon_1$  for a double quantum dot in series with  $N = 3$  energy levels in each dot ( $n = 1, 2, 3$ ). It shows that when the energy  $\varepsilon_1$  of dot 1 is aligned with  $\mu_L + \mu_R$ , here equal to zero since we set  $\mu_L = V/2$  and  $\mu_R = -V/2$ , then the value of  $\mathcal{F}_L$  at low voltage is most of the time about 0.5 or larger, excepted in some narrow purple stripes along the lines  $\varepsilon_d = n\varepsilon_0$  when  $V > 0.5$  (see left panel of Fig. 1). On the contrary, when the energy  $\varepsilon_1$  of dot 1 is not aligned with  $\mu_L + \mu_R$  (the most probable situation), one observes that the value of  $\mathcal{F}_L$  is strongly reduced at low voltage for some values of the detuning energy (see the purple color regions in the right panel of Fig. 1), leading to the possibility of reducing the noise, relatively to the current, even at low voltage. In the case of a double quantum dot arranged in parallel, the situation is opposite. Indeed, it is when the detuning energy is aligned with  $\mu_L + \mu_R$  that one observes a strong reduction of noise at low voltage (see the purple color regions in the left panel of Fig. 2), whereas for  $\varepsilon_d \neq \mu_L + \mu_R$ , one has  $\mathcal{F}_L \approx 0.5$  at low voltage (see the right panel of Fig. 2), meaning that the noise is high compared to the current. These results help to identify the regions of the  $(V, \varepsilon_d)$ -plane where one has a noise reduction.

We now turn our interest to the  $\Delta T$ -noise defined as  $\Delta\mathcal{S}_{\alpha\alpha} = \mathcal{S}_{\alpha\alpha}^{\delta T}(0) - \mathcal{S}_{\alpha\alpha}^0(0)$ , where  $\mathcal{S}_{\alpha\alpha}^{\delta T}(0)$  is the zero-frequency auto-correlator at zero voltage when the reservoir are raised to distinct temperatures, i.e.,  $T_L = T + \delta T/2$  and  $T_R = T - \delta T/2$ , and  $\mathcal{S}_{\alpha\alpha}^0(0)$  is the zero-frequency auto-correlator calculated for identical reservoir temperatures, i.e.,  $T_{L,R} = T$ . Figure 3 displays the color-scale plots of the  $\Delta T$ -noise in a double quantum dot in series for two different sets of parameters. It shows that in the regime where  $\Gamma \gtrsim T$ , the  $\Delta T$ -noise remains positive (see left panel of Fig. 3), whereas in the regime

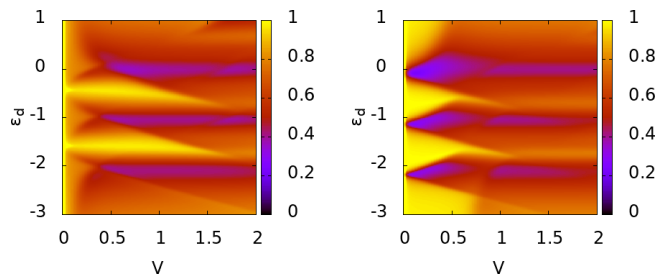


FIG. 1. Color-scale plot of the Fano factor  $\mathcal{F}_L$  as a function of the bias voltage  $V$  and the detuning energy  $\varepsilon_d$  for a double quantum dot in series, with three energy levels in each dot, equal to  $\varepsilon_{in} = \varepsilon_i + n\varepsilon_0$  where  $n = 1, 2, 3$ , with (left)  $\varepsilon_1 = 0$ , and (right)  $\varepsilon_1 = 0.3$ . The other parameters are  $\varepsilon_0 = 1$ ,  $T_{L,R} = 0.01$ ,  $\Gamma = 0.1$ , and  $\mathcal{V}_{12} = 0.2$ .

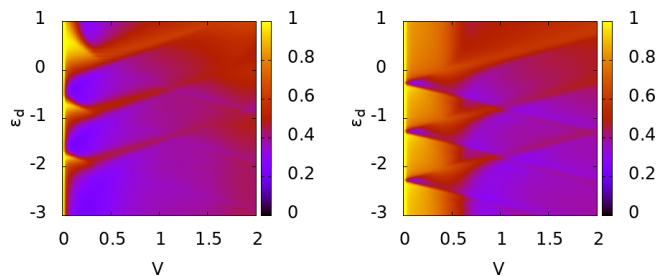


FIG. 2. Same as in Fig. 1 for a double quantum dot in parallel.

where  $\Gamma \lesssim T$ , the sign of the  $\Delta T$ -noise changes (see right panel of Fig. 3), meaning that the noise is reduced in some regions of the  $(\varepsilon_1, \varepsilon_2)$ -plane when a temperature gradient between the two reservoirs is applied. The fact that one has a change of behavior in the  $\Delta T$ -noise when reducing  $\Gamma$  is in perfect agreement with what has been obtained and generically explained in Ref. 30, with a change of behavior at  $\Gamma/T \approx 2.6$ , principally due to the fact that the energy dependencies of the transmission amplitude  $t_{\alpha\alpha}(\varepsilon)$  and transmission coefficients  $\mathcal{T}_{\alpha\alpha}(\varepsilon)$  become relevant when  $\Gamma \lesssim T$ . In the case of a double quantum dot in parallel, such a change of behavior in the  $\Delta T$ -noise, between the regime where  $\Gamma \lesssim T$  and the regime where  $\Gamma \gtrsim T$ , is also observed (see Fig. 4). In order to further understand this phenomenon, we have reported in Fig. 5 the evolution of the  $\Delta T$ -noise minimum as a function of the  $\Gamma/T$  ratio for three different quantum dot geometries: single dot, double dot in series, and double dot in parallel. We see that the value of this minimum is negative at low  $\Gamma/T$  ratio and converges to zero at  $\Gamma/T \approx 3$  whatever the geometry is. Again, this variation is in agreement with previous results on  $\Delta T$ -noise obtained for quantum systems characterized by energy-dependent transmission[30]. This is an important result because it means that there is an operating regime in which the noise can be reduced by applying a temperature gradient between the right and left reservoirs, in both single and double quantum dot systems.

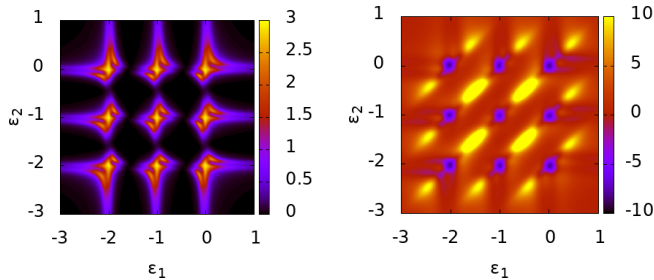


FIG. 3. Color-scale plot of the  $\Delta T$ -noise as a function of  $\varepsilon_1$  and  $\varepsilon_2$  for a double quantum dot in series (a.u.), with three energy levels in each dot, equal to  $\varepsilon_{in} = \varepsilon_i + n\varepsilon_0$  where  $n = 1, 2, 3$ , with (left)  $T = 0.01$ ,  $\Gamma = 0.1$ ,  $\mathcal{V}_{12} = 0.1$ , and (right)  $T = 0.1$ ,  $\Gamma = 0.05$ ,  $\mathcal{V}_{12} = 0.1$ . The other parameters are  $\delta T = T/2$ ,  $\varepsilon_0 = 1$ , and  $V = 0$ .

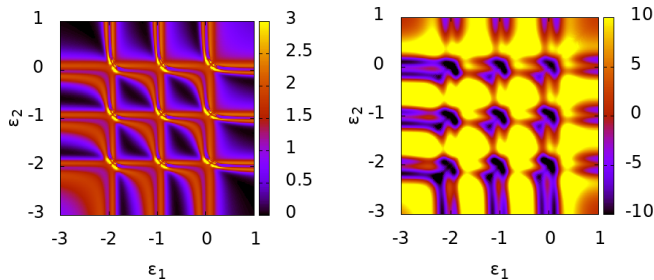


FIG. 4. Same as in Fig. 3 for a double quantum dot in parallel.

Finally, we study the finite-frequency cross-correlator for a double quantum dot in series in order to make a comparison with the experimental observations presented in Ref. 22. Figure 6 shows the cross-correlator  $\mathcal{S}_{LR}(\omega)$  near the honeycomb vertex located in the central region of the  $(\varepsilon_1, \varepsilon_2)$ -plane, at both zero-frequency ( $\omega = 0$ ) and finite-frequency ( $\omega = 0.1$ ). At zero-frequency, the cross-

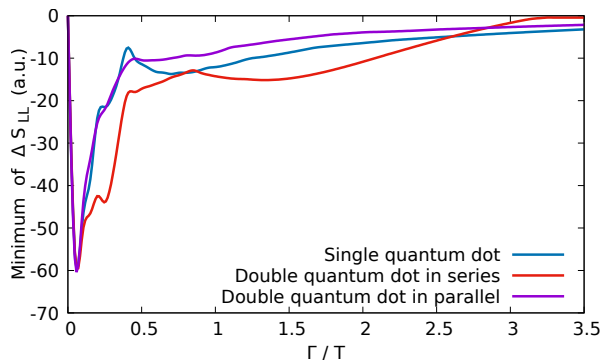


FIG. 5. Value of the minimum of the  $\Delta T$ -noise  $\Delta \mathcal{S}_{LL}$ , according to  $\varepsilon_1$  and  $\varepsilon_2$ , as a function of the ratio  $\Gamma/T$  at  $V = 0$ ,  $\mathcal{V}_{12} = 0.1$ ,  $\Gamma = 0.1$ , and  $\varepsilon_0 = 1$ . One takes  $\delta T = T/2$ . For both simple and double quantum dots, three energy levels in each dot have been included. In the parallel geometry case, a scaling factor 1/2 has been added in order to be able to compare the different curves.

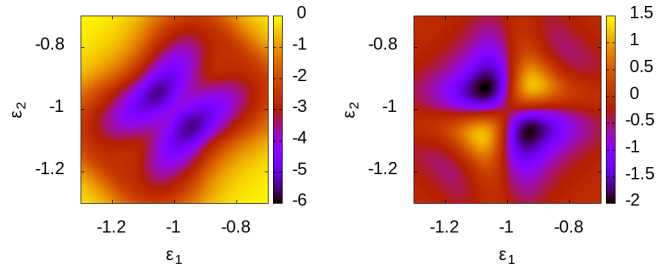


FIG. 6. Color-scale plot of the cross-correlator  $\mathcal{S}_{LR}(\omega)$  as a function of  $\varepsilon_1$  and  $\varepsilon_2$  for a double quantum dot in series (a.u.), with three energy levels in each dot, equal to  $\varepsilon_{in} = \varepsilon_i + n\varepsilon_0$  where  $n = 1, 2, 3$ , with (left)  $\omega = 0$ , and (right)  $\omega = 0.1$ . The other parameters are  $V = 0.2$ ,  $\Gamma = 0.1$ ,  $\mathcal{V}_{12} = 0.1$ ,  $T_{L,R} = 0.01$ , and  $\varepsilon_0 = 1$ .

correlator is negative in sign (see left panel of Fig. 6) as expected since one has  $\mathcal{S}_{LR}(0) = -\mathcal{S}_{LL}(0)$  with strictly positive auto-correlator, whereas at finite-frequency the sign of the cross-correlator becomes positive in some regions of the  $(\varepsilon_1, \varepsilon_2)$ -plane (see right panel of Fig. 6). Remarkably, and this deserves to be emphasized, the entire evolution of the cross-correlator that we obtained at finite-frequency is in perfect agreement with the experimental results presented in Ref. 22 which show a sign change. And identically to what is experimentally observed, one obtains a vanishing finite-frequency cross-correlator at zero voltage due to the fact that at low temperature the system can not emit noise at frequency larger than the voltage[34, 35], so that for  $\hbar\omega > eV$ , one has  $\mathcal{S}_{LR}(\omega) = \mathcal{S}_{LL}(\omega) = 0$ .

*Summary* – We have derived expressions for the auto-correlators and cross-correlators of the current fluctuations in a double quantum dot which apply to any frequency, voltage and temperature values, whatever the values of inter-dot and dot-reservoirs couplings are. They allow to highlight specific features such as the reduction of the noise and of the Fano factor, as well as the possibility of having a negative  $\Delta T$ -noise, meaning that the noise can be even more reduced by applying a temperature gradient between the two reservoirs. Moreover, it leads to behavior for the cross-correlator which is in perfect agreement with the experimental measurements[22] with a change of sign near a honeycomb vertex. The approach presented in this Letter can be extended to take electron-electron and electron-photon interactions into account, which are all the more important to be able to describe realistic situations of double quantum dot systems, as experimentally studied. Indeed, in the limit where two-electron processes are negligible compared to single-electron ones, one can insert the Green functions of the double quantum dot, calculated in the presence of interactions, into the formula we have obtained for the finite-frequency noise in order to study their effects. This has been done successfully in the case of a single quantum dot in the Kondo regime[33] and has allowed to explain

the main features of the experimental curves[36], so it would be worthwhile to do it for a double quantum dot as well.

- 
- [1] F. Martins, F. K. Malinowski, P. D. Nissen, E. Barnes, S. Fallahi, G. C. Gardner, M. J. Manfra, C. M. Marcus, and F. Kuemmeth, Noise Suppression Using Symmetric Exchange Gates in Spin Qubits, *Phys. Rev. Lett.* **116**, 116801 (2016).
- [2] E. J. Connors, J. Nelson, L. F. Edge, and J. M. Nichol, Charge-noise spectroscopy of Si/SiGe quantum dots via dynamically-decoupled exchange oscillations, *Nat Commun* **13**, 940 (2022).
- [3] B. Paquelet Wuetz, D. Degli Esposti, A. M. J. Zwerver, S. Amitonov, M. Botifoll, J. Arbiol, L. M. K. Vandersypen, M. Russ, and G. Scappucci, Reducing charge noise in quantum dots by using thin silicon quantum wells, *Nat Commun* **14**, 1385 (2023).
- [4] D. Zenelaj, P. P. Potts, and P. Samuelsson, Full counting statistics of the photocurrent through a double quantum dot embedded in a driven microwave resonator, *Phys. Rev. B* **106**, 205135 (2022).
- [5] G. Kießlich, A. Wacker, and E. Schöll, Shot noise of coupled semiconductor quantum dots, *Phys. Rev. B* **68**, 125320 (2003).
- [6] R. López, R. Aguado, and G. Platero, Shot noise in strongly correlated double quantum dots, *Phys. Rev. B* **69**, 235305 (2004).
- [7] B. H. Wu, J. C. Cao, and K.-H. Ahn, Transport through a strongly correlated quantum dot with Fano interference, *Phys. Rev. B* **72**, 165313 (2005).
- [8] J. Aghassi, A. Thielmann, M. H. Hettler, and G. Schön, Shot noise in transport through two coherent strongly coupled quantum dots, *Phys. Rev. B* **73**, 195323 (2006).
- [9] F. Bodoky, W. Belzig, and C. Bruder, Connection between noise and quantum correlations in a double quantum dot, *Phys. Rev. B* **77**, 035302 (2008).
- [10] I. Weymann, Effects of different geometries on the conductance, shot noise, and tunnel magnetoresistance of double quantum dots, *Phys. Rev. B* **78**, 045310 (2008).
- [11] B. Dong, X. L. Lei, and N. J. M. Horing, Positive current noise cross correlations in capacitively coupled double quantum dots with ferromagnetic leads, *Phys. Rev. B* **80**, 153305 (2009).
- [12] H.-F. Lü, J.-R. Zhang, T. Wu, Z. Xiao-Tao, and H.-W. Zhang, Current noise correlations in double quantum dots asymmetrically coupled to external leads, *Journal of Applied Physics* **107**, 034314 (2010).
- [13] L.-L. Zhao, H.-K. Zhao, and J. Wang, Photon-assisted Shot noise of the double quantum dot interferometer in weak Kondo regime, *Physics Letters A* **376**, 1849 (2012).
- [14] J. Luo, H. Jiao, B. Xiong, X.-L. He, and C. Wang, Spin-resolved bunching and noise characteristics in double quantum dots coupled to ferromagnetic electrodes, *Journal of Physics: Condensed Matter* **25**, 155304 (2013).
- [15] H.-F. Lü, H.-Z. Lu, and S.-Q. Shen, Enhanced current noise correlations in a Coulomb-Majorana device, *Phys. Rev. B* **93**, 245418 (2016).
- [16] P. Shi, M. Hu, Y. Ying, and J. Jin, Noise spectrum of quantum transport through double quantum dots: Renormalization and non-Markovian effects, *AIP Advances* **6**, 095002 (2016), <https://doi.org/10.1063/1.4962527>.
- [17] B. Horovitz and A. Golub, Double quantum dot scenario for spin resonance in current noise, *Phys. Rev. B* **99**, 241407 (2019).
- [18] N. Maslova, P. Arseyev, and V. Mantsevich, Tunneling current and noise of entangled electrons in correlated double quantum dot, *Sci Rep* **11**, 9336 (2021).
- [19] H. Sun and G. Milburn, A new approach to current and noise in double quantum dot systems, *Physica E: Low-dimensional Systems and Nanostructures* **6**, 664 (2000).
- [20] B. H. Wu and J. C. Cao, Interference of conductance and shot noise properties of photon-assisted transport through a T-shaped double quantum dot, *Phys. Rev. B* **73**, 205318 (2006).
- [21] N. Lambert, R. Aguado, and T. Brandes, Nonequilibrium entanglement and noise in coupled qubits, *Phys. Rev. B* **75**, 045340 (2007).
- [22] D. T. McClure, L. DiCarlo, Y. Zhang, H.-A. Engel, C. M. Marcus, M. P. Hanson, and A. C. Gossard, Tunable Noise Cross Correlations in a Double Quantum Dot, *Phys. Rev. Lett.* **98**, 056801 (2007).
- [23] S. Singh, E. Roldán, I. Neri, I. M. Khaymovich, D. S. Golubev, V. F. Maisi, J. T. Peltonen, F. Jülicher, and J. P. Pekola, Extreme reductions of entropy in an electronic double dot, *Phys. Rev. B* **99**, 115422 (2019).
- [24] J. Rech, T. Jonckheere, B. Grémaud, and T. Martin, Negative  $\Delta-T$  Noise in the Fractional Quantum Hall Effect, *Phys. Rev. Lett.* **125**, 086801 (2020).
- [25] M. Hasegawa and K. Saito,  $\Delta-T$  noise in the Kondo regime, *Phys. Rev. B* **103**, 045409 (2021).
- [26] G. Rebora, J. Rech, D. Ferraro, T. Jonckheere, T. Martin, and M. Sasseti,  $\Delta-T$  noise for fractional quantum Hall states at different filling factor, *Phys. Rev. Res.* **4**, 043191 (2022).
- [27] A. Popoff, J. Rech, T. Jonckheere, L. Raymond, B. Grémaud, S. Malherbe, and T. Martin, Scattering theory of non-equilibrium noise and delta T current fluctuations through a quantum dot, *Journal of Physics: Condensed Matter* **34**, 185301 (2022).
- [28] E. Zhitlukhina, J. Rech, M. Belogolovskii, and P. Seidel, Low Temperature Probing of On-Surface Dynamical Fluctuations with Johnson-Nyquist and  $\Delta-T$  Noises, *J. of Low Temp. Phys.* (2023).
- [29] M. Hübler and W. Belzig, Light emission in  $\Delta-T$ -driven mesoscopic conductors, *Phys. Rev. B* **107**, 155405 (2023).
- [30] G. Zhang, I. V. Gornyi, and C. Spånslätt,  $\Delta-T$  noise for weak tunneling in one-dimensional systems: Interactions versus quantum statistics, *Phys. Rev. B* **105**, 195423 (2022).
- [31] M. Lavagna, V. Talbo, T. Q. Duong, and A. Crépieux, Level anticrossing effect in single-level or multilevel double quantum dots: Electrical conductance, zero-frequency charge susceptibility, and Seebeck coefficient, *Phys. Rev. B* **102**, 115112 (2020).
- [32] R. Zamoum, M. Lavagna, and A. Crépieux, Nonsymmetrized noise in a quantum dot: Interpretation in terms of energy transfer and coherent superposition of scattering paths, *Phys. Rev. B* **93**, 235449 (2016).
- [33] A. Crépieux, S. Sahoo, T. Q. Duong, R. Zamoum, and M. Lavagna, Emission Noise in an Interacting Quantum Dot: Role of Inelastic Scattering and Asymmetric Cou-

- pling to the Reservoirs, *Phys. Rev. Lett.* **120**, 107702 (2018).
- [34] R. Aguado and L. P. Kouwenhoven, Double Quantum Dots as Detectors of High-Frequency Quantum Noise in Mesoscopic Conductors, *Phys. Rev. Lett.* **84**, 1986 (2000).
- [35] R. Deblock, E. Onac, L. Gurevich, and L. Kouwenhoven, Detection of Quantum Noise from an Electrically Driven Two-Level System, *Science* **301**, 203 (2003).
- [36] R. Delagrangé, J. Basset, H. Bouchiat, and R. Deblock, Emission noise and high frequency cut-off of the Kondo effect in a quantum dot, *Phys. Rev. B* **97**, 041412 (2018).